



OPEN

Understanding ultrafine nanodiamond formation using nanostructured explosives

Vincent Pichot¹, Benedikt Risse¹, Fabien Schnell¹, Julien Mory² & Denis Spitzer¹

¹NS3E «Nanomatériaux pour les Systèmes Sous Sollicitations Extrêmes» UMR ISL-CNRS-UDS 3208, French-German Research Institute of Saint-Louis, 5 rue du Général Cassagnou 68301 Saint-Louis, France, ²French-German Research Institute of Saint-Louis, 5 rue du Général Cassagnou 68301 Saint-Louis, France.

The detonation process is able to build new materials with a bottom-up approach. Diamond, the hardest material on earth, can be synthesized in this way. This unconventional synthesis route is possible due to the presence of carbon inside the high-explosive molecules: firing high-explosive mixtures with a negative oxygen balance in a non-oxidative environment leads to the formation of nanodiamond particles. Trinitrotoluene (TNT) and hexogen (RDX) are the explosives primarily used to synthesize nanodiamonds. Here we show that the use of nanostructured explosive charges leads to the formation of smaller detonation nanodiamonds, and it also provides new understanding of nanodiamond formation-mechanisms. The discontinuity of the explosive at the nanoscale level plays the key role in modifying the diamond particle size, and therefore varying the size with microstructured charges is impossible.

Synthesis of detonation nanodiamonds involves the following four research areas: decrease in particle size, control of particle aggregation during synthesis, optimization of functional surface groups, and controlled doping of such particles¹. The conditions surrounding the synthesis of nanodiamonds have already been investigated with a view to controlling particle-size, and modifying the reaction environment and the configuration of the explosive charges only had a slight influence on the nanodiamond particle-size²⁻⁵. Research into the synthesis of detonation nanodiamonds began in the USSR in the Sixties and was later developed in other countries⁶.

The unique properties of the nanodiamond—hardness, thermal conductivity, biocompatibility, photoluminescence, surface chemistry, electrical insulation—make it a very attractive material for various applications⁷. Medicine⁷⁻⁹, magnetometry¹⁰⁻¹² and sensors¹³ are only some of the many fields with applications where nanodiamonds may lead to groundbreaking innovations. Although the intrinsic properties of diamonds are already of great interest, the main breakthrough should arise from the size of nanodiamond particles⁵. The smallest nanoparticles are of great importance for fundamental and applicative research. Their physical and chemical properties can be modified according to their intended applications. For diamonds with a size smaller than 2 nm, theoretical works predict quantum confinement effects due to an increase in the band gap¹⁴. The diamond nanoparticles may help understanding the appearance and the evolution of these quantum effects when decreasing the size of the particles. The ability to use these particles as quantum dots in applications such as quantum computers, cryptography or medical imagery can enable major progress in numerous scientific domains.

The detonation of high-explosive mixtures with a negative oxygen balance leads to the formation of nanodiamonds with sizes of between 2 and 20 nanometres. Their size distributions have a lognormal shape centred at 4 to 5 nm and with a long trailing edge. When in suspension, only a very small fraction (0.01 wt%) of the smallest nanodiamonds (i.e. particle sizes of between 2 and 4 nanometres) can be isolated by ultracentrifugation¹⁵.

Despite intensive research focused on the understanding of the diamond-formation process, its fundamental mechanisms are still subject to discussion^{2-4,16-20}. Various possible mechanisms based on thermodynamic assumptions, and the evaluation of the final product, were used to explain the nanodiamond formation-mechanisms during the detonation process^{4,17-19}. Remarkable works on the subject of nanodiamond formation accomplished by Titov and co-workers based on in-situ measurements using synchrotron radiation^{3,16,20} have investigated the detonation process.

Here we propose a pioneering approach which uses nanostructured explosive charges for the synthesis of smaller nanodiamonds. Due to the nanostructure of the explosive, the grain boundaries form a discontinuity in

SUBJECT AREAS:

NANOPARTICLES

SYNTHESIS AND PROCESSING

MATERIALS SCIENCE

NANOSCALE MATERIALS

Received
22 March 2013Accepted
20 June 2013Published
8 July 2013

Correspondence and requests for materials should be addressed to D.S. (denis.spitzer@isl.eu)



the explosive matrix on a very small scale which strongly influences the quality of the synthesized nanodiamonds. These novel experiments have provided new insight into the comprehension of nanodiamond formation.

Results

Microstructured and nanostructured hexolites composed of 60 wt% of hexogen and 40 wt% of trinitrotoluene were chosen as the explosive formulation due to the fact that they provide the highest nanodiamond output. By means of careful preparation, explosive pressed charges with the same composition (60.2/39.8) and the same density (1.67 g.cm^{-3}) were obtained. Scanning Electron Microscopy (SEM) images of the explosive charges shown in Fig. 1 reveal a strong difference between microstructured and nanostructured explosive charges.

The microstructured charge exhibits large TNT and RDX particles with sizes between 5 and 100 μm , while in the nanostructured charge the particle size is between 50 and 200 nm.

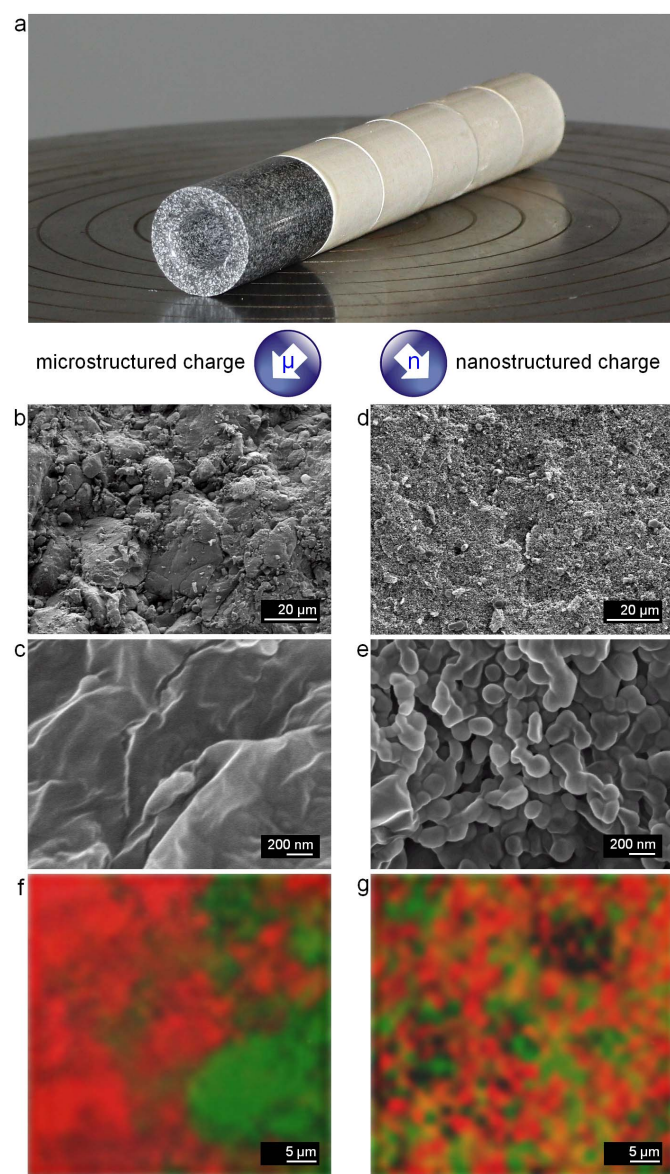


Figure 1 | Explosive charge structures. (a), Photograph of the explosive charge. (b–e), SEM micrographs of the microstructured (b–c) and nanostructured (d–e) explosive pellets showing enlarged views of the samples. (f–g), Raman mapping of the microstructured (f) and nanostructured (g) explosive pellets.

Using Raman spectroscopy, RDX and TNT can be differentiated by means of their spectral signatures. The intensity of the signal located at 1618 cm^{-1} corresponding to the C=C aromatic stretching vibration in TNT, and the band at 1272 cm^{-1} corresponding to the N-O stretching in RDX, have been selected to indicate the distribution of both explosives in the different samples^{21,22}.

Raman spectroscopy mapping shows a much more homogeneous distribution of RDX and TNT in the nanostructured charge than in the microstructured charge (Fig. 1f and 1g). The TNT (green) and RDX (red) signals reveal a uniform distribution of both components in the nanostructured charge, whereas the microstructured charge is dominated by micron-sized TNT and RDX regions. Due to the limiting resolution of Raman spectroscopy, individual RDX and TNT particles could not be discriminated by this technique. Certain Raman spectra may result from the superposition of multiple particles; however, this technique does reveal the homogeneity degree of the explosive charges.

X-Ray Diffraction (XRD) patterns of the microstructured and nanostructured hexolites are quite similar (Fig. 2), indicating that the nanohexolite is composed of individual TNT and RDX particles and neither co-crystallization nor core-shell structures occurred. It can be noticed that an enlargement of the diffraction peaks of TNT and RDX is observed, indicating finer elementary crystallites in the case of nanostructured hexolite.

After firing both charges, detonation soot was recovered and characterized. Transmission Electron Microscopy (TEM) images clearly show that smaller nanodiamonds were formed by the nanostructured charge (Fig. 3).

Particle-size distribution curves from the collected nanodiamonds were obtained for the nanostructured and the corresponding microstructured charge by a careful statistical evaluation of the size of more than 500 individual particles for each sample (the dimensions of nanodiamonds were manually measured by 4 different persons, ensuring the validity of the results). The nanodiamond particle-size distribution obtained from the nanostructured hexolite is narrower and therefore more homogeneous than in the case of the microstructured charge, in which nanodiamonds with sizes of over 10 nm can be obtained. Their mean particle diameters are 4.2 and 6.3 nm respectively. In both cases, lognormal law allows representation of particle size distribution.

The cumulative frequencies were calculated from the size distribution data of both samples. Two main results can be highlighted:

- For the nanostructured charge, the fraction of nanodiamonds having a size of below 3 nm is nearly 20%, in contrast to only 4% of those formed by the microstructured charge.

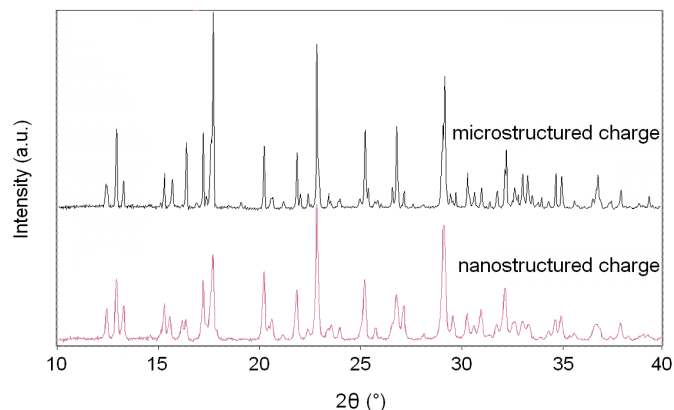


Figure 2 | Diffraction patterns of explosive materials. XRD patterns of nanostructured (red) and microstructured (black) hexolites.

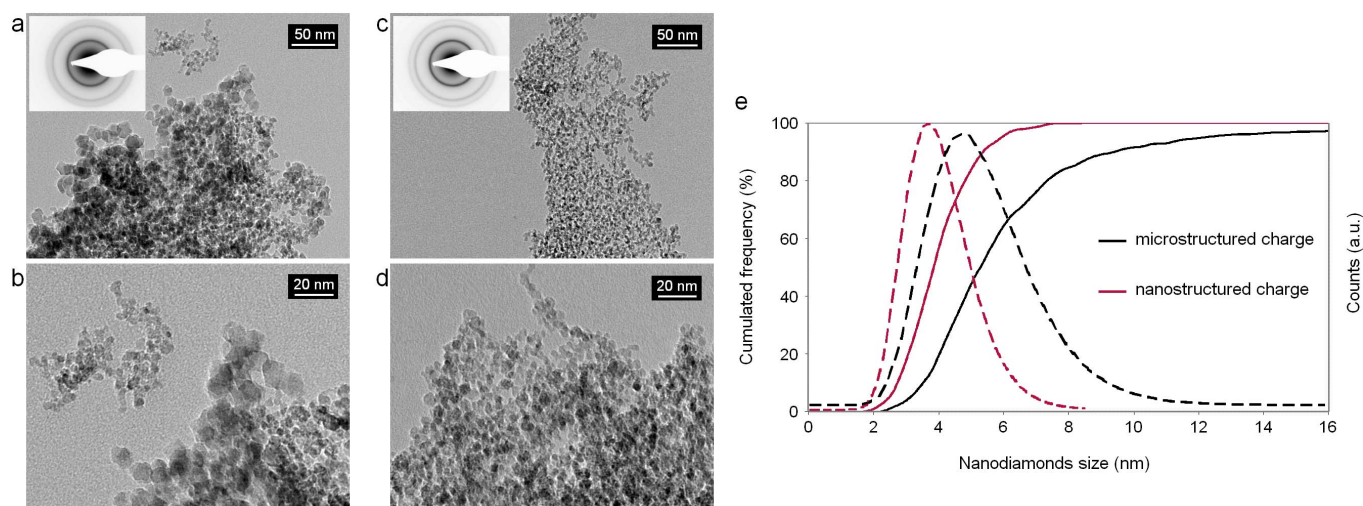


Figure 3 | Nanodiamonds synthesized from nanostructured and microstructured explosives. (a–d), TEM micrographs showing nanodiamonds obtained from microstructured (a, b) and nanostructured (c, d) explosive charges. Inset in (a and c) Electronic diffraction patterns showing the diffraction ring of the (111), (220), and (311) diamond planes ($d_{hkl} = 0.207$ nm, 0.125 nm, 0.107 nm). (e), Size distributions and cumulative frequencies for both samples.

- The largest nanodiamonds formed by the nanostructured charge have a size of about 8 nm, whereas in the microstructured charge, nanodiamonds with sizes up to 23 nm could be found.

XRD experiments were conducted on the obtained nanodiamonds, the elementary crystallite sizes were measured by using the Scherrer equation on the diffraction peak of the (111) planes of diamond giving 2.9 nm and 4.7 nm for the nanodiamonds synthesized by the nanostructured and the microstructured explosive charge respectively. By taking into account the fact that there may be one graphitic layer or fullerene-like structure on the nanodiamond surface, 0.6 nm in diameter have to be added to the diamond crystalline particle measured by XRD, leading to particle sizes of 3.5 and 5.3 nm respectively which is in good agreement with the mean size of the size distribution.

Dynamic Light Scattering (DLS) measurements were performed on suspended nanodiamond samples (Fig. 4a), indicating a smaller and narrower particle size distribution in the case of the nanodiamonds synthesized by the nanostructured explosive. Atomic Force Microscopy (AFM) measurements were achieved on ultracentrifuged suspensions in order to definitely prove that the proportion of finest nanodiamond particles was significantly higher in the sample synthesized from nanostructured explosive charge (Fig. 4b). The density of individual small particles is around 50 times higher in the case of the nanodiamonds synthesized by the nanostructured explosive indicating that these nanodiamond particles are easier to deaggregate by conventional techniques.

Numerous studies investigated the size dependent of the nanodiamond particles^{14,23–25}. Barnard and collaborators found that the higher stability of nanodiamond particles is in the range of approximately 1.9 – 5.2 nm²³. Ab initio calculations showed that for nanodiamond with sizes up to 1 nm, dehydrogenated octahedral and cuboctahedral nanodiamonds represent unstable morphologies leading to preferential graphitization and exfoliation of the (111) surface²⁴. Raty and coworkers calculations showed that nanodiamonds with size in the 2–4 nm range exhibit a hybrid structure called bucky diamond made of nanodiamond core and a fullerene-like surface¹⁴. Raty also demonstrates by ab initio calculations that for nanodiamonds with sizes down to 3 nm it is energetically more favorable to have a bare, reconstructed surface rather than hydrogenated surface²⁵. In the light of these works, it is clear that the smallest nanodiamond with sizes down to 2 nm can be energetically stable. The nanodiamond particles are probably covered by fullerene-like

structure, further investigations will be carried out in order to determine the surface structure of the nanodiamonds on a local scale.

All the previous results clearly demonstrate the advantages of nanostructured explosive charges over microstructured charges, particularly in the formation of smaller nanodiamonds and the

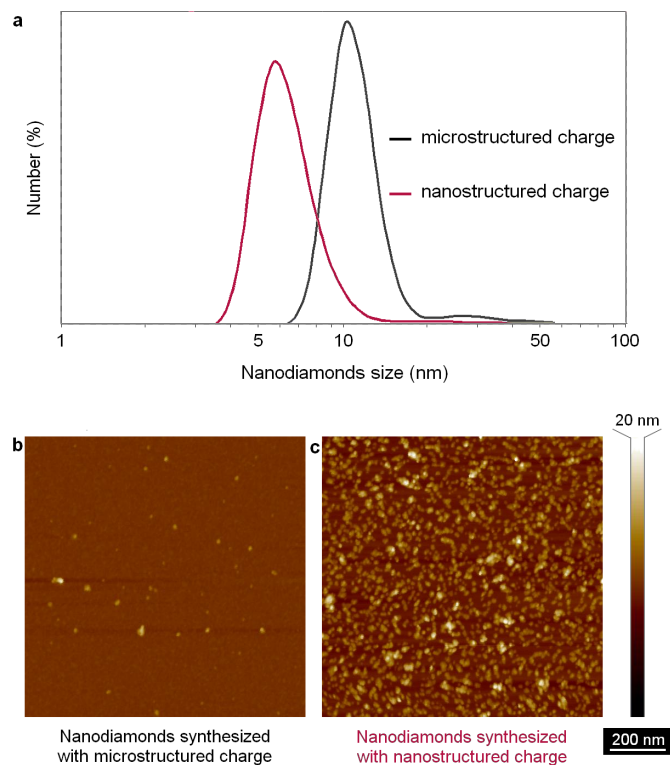


Figure 4 | Analysis of the nanodiamond particle sizes. (a), DLS measurements on nanodiamond suspensions prepared from nanodiamonds obtained by detonation of nanostructured explosive charge (red) and microstructured one (black). (b–c), AFM images obtained from supernatant of nanodiamond suspension submitted to ultrasonic stirring and ultracentrifugation, (b), nanodiamonds synthesized from microstructured explosive charge, (c), nanodiamonds synthesized from nanostructured explosive charge.



obtaining of narrower particle-size distribution. This striking discovery furthers understanding of this type of synthesis as it opens the synthesis route for ultra-small detonation nanodiamonds for use in various target applications such as quantum computers, biology, electronics and optonics which necessitate ultra-small diamonds.

The studied nanostructured explosive and further nanostructured formulations were prepared by means of the nanocrystallization process^{26,27}. Depending on the RDX/TNT ratio in the initial solution, the particle size of the nanostructured explosive varied. While hexolite 40/60 and 60/40 have a median particle size centred at 100 nm, the hexolite 80/20 reveals noticeably larger particles with occasional particles reaching sizes of up to 1 μm (Fig. 5). It was observed that the higher the TNT ratio in the explosive composition, the smaller the resulting explosive particles. For both 40/60 and 60/40 ratios, the explosive particles exhibit very narrow size distributions. Nanodiamonds synthesized from these nanostructured explosive formulations are very similar in size and distribution, whereas with the 80/20 ratio, the cumulative frequency exhibits larger particles which are comparable with the nanodiamonds obtained from the 60/40 microstructured charge.

Until now, different research groups worldwide have performed the detonation nanodiamond synthesis using classic micron-sized explosives. These explosive charges are usually obtained through one of two different processes:

- Compression of micrometric TNT and RDX grains with the eventual adding of a binder in order to improve its mechanical characteristics.
- Casting in which micrometric RDX is dispersed in molten TNT at about 85°C. After the homogenization of the mixture, the dispersion is allowed to slowly cool down to room temperature.

In both cases, the explosive matrix was composed of individual particles and cross-linked structures which were larger than ten micrometers.

Discussion

In 1989, Titov and co-workers studied the formation-mechanisms of nanodiamonds and raised the question of the influence of the homogeneity of the high-explosive mixture². At the moment of detonation, the thickness of the relevant diffusion layer for carbon clusters was calculated to be of around 0.6 μm for 1 nm nuclei at 3000 K and a reaction time of 0.5 μs . Because of the small thickness of the diffusion layer compared to the micron-sized dimensions of the explosive matrix (5 to 100 microns), the formation of the nanodiamonds occurred independently of the composition and structure of the explosive charge. In this case, the diffusion zone, being noticeably smaller than the particle size, represents only a small fraction within an explosive particle.

In our case, the preparation of the charge was performed by pressing the nanostructured explosive at room temperature in order to preserve the nanostructure. Reverting to the thesis of Titov, the diffusion zone in our case comprises several individual particles of TNT and RDX.

As the TNT contains a high number of carbon atoms, it is widely accepted that most of the carbon atoms forming the detonation nanodiamonds originate from this molecule. In the nanostructured explosive charge, the TNT particles are of nanometric or submicrometric size. In the instant of decomposition, the diffusion of the carbon nuclei will be inhibited by the grain boundary of the TNT particle and the reaction products of neighbouring RDX particles which also act as a diffusion barrier.

Therefore, the interactions of the TNT decomposition products are limited to a single TNT particle and so limit the size of the resulting nanodiamond particles. In the case of nanostructured explosives, the diffusion zone is limited to the size of the explosive particles (Fig. 6), due to the discontinuity of the explosive charge at the nanometric scale.

In the case of the 80/20 hexolite charge, particles with sizes around 600 nm were observed (Fig. 3), being close to the size of the diffusion

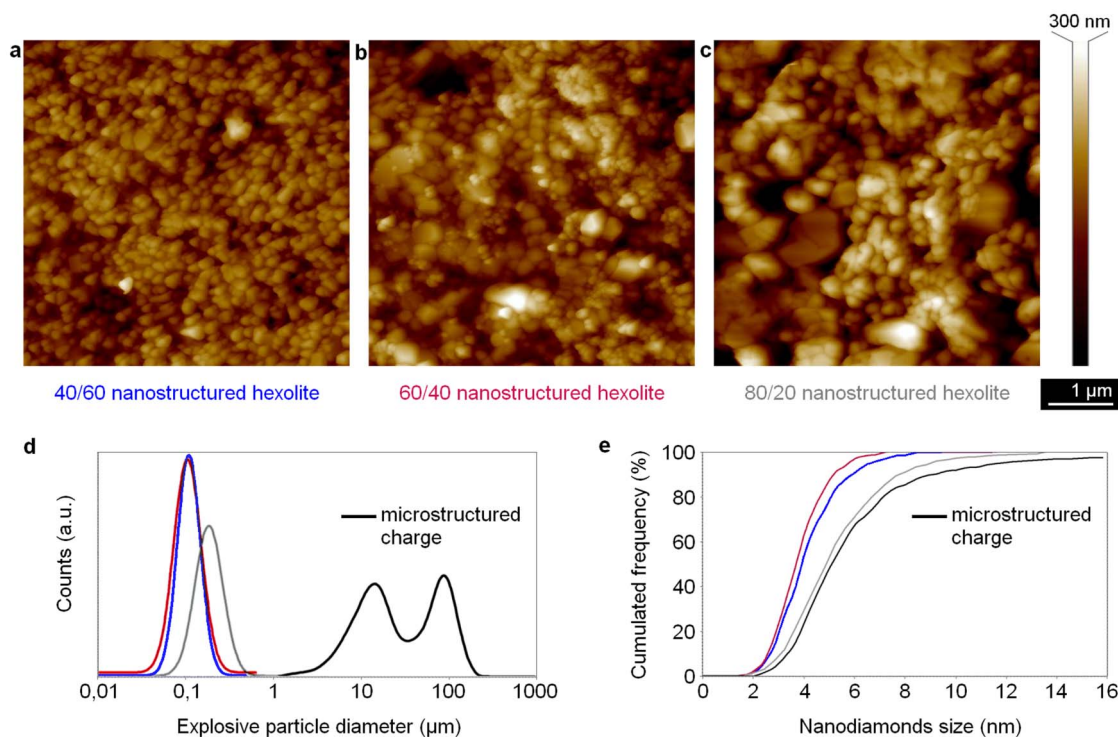


Figure 5 | Nanostructured explosives and the corresponding synthesized nanodiamonds. (a–c), AFM micrographs of the 40/60 (a), 60/40 (b) and 80/20 (c) nanostructured hexolite. (d), Size distribution of the three nanostructured explosives. (e), Cumulative frequencies of the nanodiamond sizes obtained from each explosive charge.

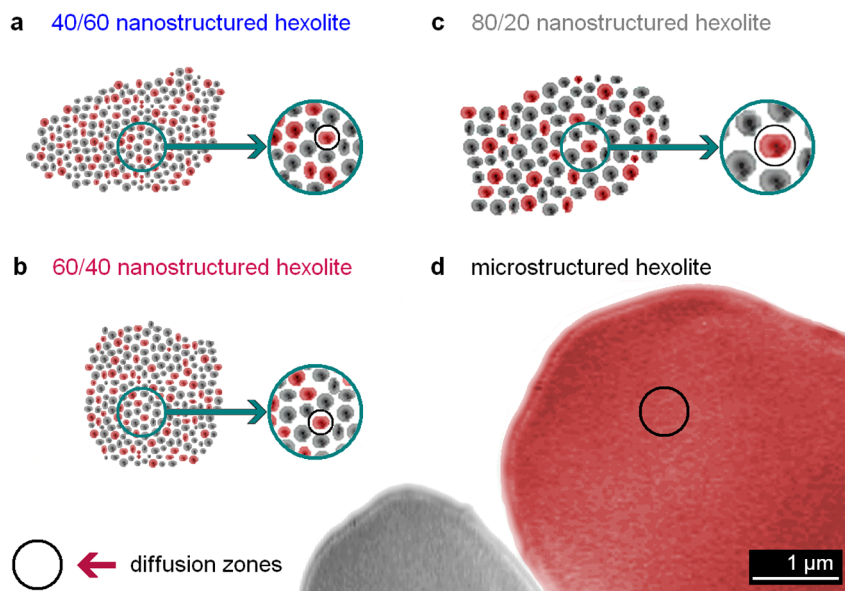


Figure 6 | Diffusion zone for nanostructured and microstructured explosive charges. (a–c), Nanostructured hexolites. (d), Microstructured hexolite. The red and the grey particles are TNT and RDX respectively. The black circles indicate the actual diffusion zone. For nanostructured explosives the diffusion zone is limited to the size of one TNT particle due to the discontinuity of the charge.

zone described by Titov. Larger diamond nanoparticles, with a size close to the diamonds obtained from the microstructured charge, were obtained. This last result corroborates the diffusion zone model.

A comparison of nanodiamond syntheses using nanostructured and microstructured explosives was performed. The detonation of a nanostructured explosive charge formed smaller nanodiamonds than those synthesized by a microstructured charge. Moreover, these experiments allowed the development of a new approach to the understanding of the mechanisms which form detonation nanodiamonds. Indeed, we have proven that a direct relation exists between the size of the explosive particles and the size of the synthesized nanodiamonds.

These results have two major consequences: First, the synthesis of very small nanodiamonds will open new opportunities and lead to breakthroughs in various disciplines. The second concerns the understanding of detonation mechanisms on the nanoscale. Until now, detonation theory was only considered on a macroscopic scale; this novel approach should give new insights into the properties of nano-explosives and the mechanisms involved during detonation.

This approach can also be applied to other materials, nano-oxides for instance, which are obtained via the bottom-up detonation synthesis route.

Methods

Preparation of hexolites. The preparation of nanostructured hexolite was achieved through the flash-evaporation process, a nanocrystallization technique developed at the ISL^{26,27}. The nanostructuring and the mixing of the components occur simultaneously, and a homogeneous distribution of both explosives is obtained in the final product.

All types of nanostructured hexolite with varying ratios of RDX and TNT were prepared in the same manner from a 1 wt% acetone-explosive solution. While the total mass of the dissolved material remained constant, the ratio of RDX to TNT was changed accordingly.

Using an overpressure of 40 bars, the acetone-explosive solution was atomized into a vacuum atomization chamber by means of a hollow cone nozzle with a 60 μm nozzle-diameter. The temperature of the nozzle was kept constant at 160°C. A vacuum pump maintained a constant pressure of 5 mbar in the atomization chamber.

Applying such a high temperature to the acetone-explosive solution causes its instantaneous evaporation once it is atomized into the vacuum atomization chamber. The crystallized explosive particles were separated from the gas flow by means of two parallel axial cyclones, which were used alternately to enable continuous operation. The ratio of RDX to TNT was unaffected by the nanocrystallization process. The micron-sized hexolite was prepared by physically mixing micron-sized RDX and TNT for 30 minutes by using a rotating mechanical agitator.

Charges and firing. For each explosive charge, five pellets with lengths and diameters of 15.8 mm ($L/\Phi = 1$) were obtained through compression of pulverent hexolite at room temperature for 10 minutes in order to obtain the same density (1.67 g cm^{-3}). These pellets were cemented together using pyrotechnic glue to form the final explosive charge. The explosive charges were placed in a water-filled pocket and fired inside a detonation tank.

Hexolite and nanodiamond characterization. The morphologies of the hexolites were observed by Scanning Electron Microscopy (5 kV, DSM 982 Gemini SEM, Zeiss) and by Atomic Force Microscopy (Nanoscope IV, atomic force microscope, Veeco Metrology Group) using a Veeco 'RTESP' (Rotated Tip Etched Silicon Probe) AFM probe. This probe has a silicon cantilever with a length of 125 μm, a width of 35 μm and a thickness of 4 μm. The tip has a curvature radius of about 10 nm. SEM was mainly chosen for a large general view of the sample, as the SEM conditions may partially deteriorate the explosive particles. AFM measurements were performed in order to determine the real particle size and morphology of the nanostructured explosives. Concerning nanodiamonds imaging by AFM, a Veeco 'FESP' (Force Etched Silicon Probe) AFM probe was used, the nanodiamonds were deposited on atomically flat mica. Raman spectroscopy was conducted with a Renishaw in Via Raman microscope equipped with a 514 nm laser. XRD was performed on a Bruker D8 Advance powder diffraction spectrometer with $\text{Cu K}\alpha_1$ radiation ($\lambda = 0.154 \text{ nm}$). Transmission Electron Microscopy (TEM) micrographs and electronic diffraction were obtained with a Philips CM200. Suspensions of nanodiamonds synthesized from nanostructured and microstructured hexolites (60/40) were prepared at a concentration of 1 g L^{-1} and submitted to one hour of ultrasonic stirring and ultracentrifugation. The size distributions of the nanodiamonds present in the supernatant of the resulting suspensions were analyzed by Dynamic Light Scattering (Malvern zetazizer NanoZS).

1. Ho, D. *Nanodiamond Applications in Biology and Nanoscale Medicine* Ch. 4 (Springer, New York, 2010).
2. Titov, V. M., Anisichkin, V. F. & Mal'kov, I. Yu. Synthesis of ultradispersed diamond in detonation waves. *Combustion, Explosion and Shock Waves* **25**, 372–379 (1989).
3. Titov, V. M., Tolochko, B. P., Ten, K. A., Lukyanchikov, L. A. & Zubkov, P. I. The formation kinetics of detonation nanodiamonds in *Synthesis. Properties and Applications of Ultrananocrystalline Diamond* 169–180 (Springer, Dordrecht, 2005).
4. Danilenko, V. V. Specific features of synthesis of detonation nanodiamonds. *Combustion Explosion and Shock Waves* **41**, 577–588 (2005).
5. Kuznetsov, V. L. *et al.* Effect of explosion conditions on the structure of detonation soots: ultradisperse diamonds and onion carbon. *Carbon* **32**, 873–882 (1994).
6. Danilenko, V. V. On the history of the discovery of nanodiamond synthesis. *Physics of the Solid State* **46**, 595–599 (2004).
7. Mochalin, V. N., Shenderova, O., Ho, D. & Gogotsi, Y. The properties and applications of nanodiamonds. *Nature Nanotech* **7**, 11–23 (2012).
8. Huang, H., Pierstorff, E. & Ho, D. Protein-mediated assembly of nanodiamond hydrogels into a biocompatible and biofunctional multilayer nanofilm. *ACS Nano* **2**, 203–212 (2008).



9. Ho, D. Beyond the sparkle: The impact of nanodiamonds as biolabeling and therapeutic agents. *ACS Nano* **3**, 3825–3829 (2009).
10. Waldherr, G. *et al.* High-dynamic-range magnetometry with a single nuclear spin in diamond. *Nature Nanotech* **7**, 105–108 (2012).
11. Nusran, N. M., Momeen, M. U. & Dutt, M. V. G. High-dynamic-range magnetometry with a single electronic spin in diamond. *Nature Nanotech* **7**, 109–113 (2012).
12. Balasubramanian, G. *et al.* Nanoscale imaging magnetometry with diamond spins under ambient conditions. *Nature* **455**, 648–651 (2008).
13. Maletinsky, P. *et al.* A robust scanning diamond sensor for nanoscale imaging with single nitrogen-vacancy centres. *Nature Nanotech* **7**, 320–324 (2012).
14. Raty, J.-Y., Galli, G., Bostedt, C., van Buuren, T. W. & Terminello, L. J. Quantum confinement and fullerene-like surface reconstruction in nanodiamonds. *Phys. Rev. Lett.* **90**, 037401 (2003).
15. Schmidlin, L. *et al.* Two-dimensional nanodiamond monolayers deposited by combined ultracentrifugation and electrophoresis techniques. *App. Phys. Lett.* **101**, 253111 (2012).
16. Titov, V. M., Tolochko, B. P., Ten, K. A., Lukyanichikov, L. A. & Prueel, E. R. Where and when are nanodiamonds formed under explosion? *Diam. Relat. Mater.* **16**, 2009–2013 (2007).
17. Anischkin, V. F. Isotope Studies of Detonation Mechanisms of TNT, RDX, and HMX. *Combustion, Explosion, and Shock Waves* **43**, 580–586 (2007).
18. Kozyrev, N. V. & Golubeva, E. S. Investigation of the synthesis of ultradispersed diamonds in mixtures of TNT with RDX, HMX and PETN. *Combustion, Explosion, and Shock Waves* **28**, 560–564 (1992).
19. Malkov, I. Yu. *et al.* Formation of diamond from the liquid phase carbon. *Combustion, Explosion, and Shock Waves* **29**, 542–544 (1993).
20. Chernishev, A. P. *et al.* Physical–chemical model of nanodiamond formation at explosion. *Nuclear Instruments and Methods in Physics Research A* **575**, 72–74 (2004).
21. Wang, X. *et al.* Detection of TNT in acetone using Raman spectroscopic signature. *Proc. Of International Symposium on Photoelectronic Detection and Imaging 2007: Laser, Ultraviolet, and Terahertz Technology*, edited by Liwei Zhou, Proc. of SPIE Vol. 6622, 662219 (2008) doi: 10.1117/12.790827.
22. Karpowicz, R. J. & Brill, T. B. Comparison of the molecular structure of hexahydro-1,3,5-trinitro-s-triazine in the vapor, solution and solid phases. *J. Phys. Chem.* **88**, 348–352 (1984).
23. Barnard, A. S., Russo, S. P. & Snook, I. K. Size dependent phase stability of carbon Nanoparticles: nanodiamond versus fullerenes. *J. Chem. Phys.* **118**, 5094–5097 (2003).
24. Barnard, A. S., Russo, S. P. & Snook, I. K. Structural relaxation and relative stability of nanodiamond morphologies. *Diam. Relat. Mater.* **16**, 1867–1872 (2003).
25. Raty, J. Y. & Galli. Ultradispersity of diamond at the nanoscale. *Nat. Mater.* **2**, 792–795 (2003).
26. Risse, B. *et al.* Continuous formation of submicron energetic particles by the flash-evaporation technique. *Chem. Eng. J.* **203**, 158–165 (2012).
27. Risse, B., Spitzer, D. & Hassler, D. Patent, FR 1251143, Préparation de nanoparticules d'explosif par évaporation flash.

Acknowledgements

Loïc Vidal at the “Institut de Science des Matériaux de Mulhouse” (IS2M), for the TEM micrographs.

Author contributions

D.S. conceived the original idea and D.S. and V.P. directed the research. B.R. synthesized the nanostructured explosives and made the Raman spectroscopy experiments. J.M. prepared the explosive charges. F.S. performed the SEM experiments on the explosive samples. V.P. conducted the AFM experiments on explosive nanoparticles, synthesized the nanodiamond particles. All authors participated to the analysis of the data and discussed the results. V.P. and D.S. wrote the paper, and all authors provided their feedback.

Additional information

Competing financial interests: The authors declare no competing financial interests.

How to cite this article: Pichot, V., Risse, B., Schnell, F., Mory, J. & Spitzer, D. Understanding ultrafine nanodiamond formation using nanostructured explosives. *Sci. Rep.* **3**, 2159; DOI:10.1038/srep02159 (2013).



This work is licensed under a Creative Commons Attribution-NonCommercial-NoDerivs 3.0 Unported license. To view a copy of this license, visit <http://creativecommons.org/licenses/by-nc-nd/3.0>